

Exploration of synergism between a polymer matrix and gold nanoparticles for selective determination of dopamine

S. Senthil Kumar, J. Mathiyarasu, K. Lakshminarasimha Phani *

Electrodeposition & Electrocatalysis Division, Central Electrochemical Research Institute, Karaikudi 630 006, Tamil Nadu, India

Received 19 August 2004; received in revised form 6 December 2004; accepted 7 December 2004

Available online 5 February 2005

Abstract

In this work, synergism between the conducting polymer matrix and gold nanoparticles is explored for dopamine sensing in the presence of excess ascorbic acid using poly (3,4-ethylenedioxythiophene) (PEDOT) in neutral phosphate buffer solutions (PBS 7.4). The electrodeposited thin films of PEDOT were characterized by atomic force microscopy (AFM) (and current sensing-AFM), and the incorporated Au nanoparticles by UV-Vis spectroscopy and electrochemical methods. Distinct “oxidized” and “reduced” regions of the polymer film were revealed in the CS-AFM. Electrochemical studies have shown that the catalytic oxidation of DA and AA on PEDOT modified electrodes can afford a peak potential separation of ~ 230 mV. Further enhancement in the oxidation current for DA/AA oxidation was achieved by incorporation of Au nanoparticles in the PEDOT modified electrodes. The nanometer sized gold particles favour the nanomolar sensing of dopamine in the presence of excess of ascorbic acid (1.0 mM). The DA oxidation current increases linearly with DA concentration and the detection limit of DA is found to be ~ 2 nM. Amperometric detection under stirred conditions is free from electrode fouling at lower concentrations of DA and is only slightly affected at concentrations beyond $20 \mu\text{M}$. The combined effect of Au nanoparticles and the PEDOT matrix is based on the Au_{nano} surrounded by a “hydrophobic sheath” tending to reside within these hydrophobic regions of PEDOT, increasing the DA oxidation current.
© 2005 Elsevier B.V. All rights reserved.

Keywords: Atomic force microscopy; Cyclic voltammetry; Amperometric sensor; Electrocatalytic oxidation; Conducting polymer; Chemically modified electrode

1. Introduction

Dopamine (DA), the most important among the class of catecholamines, plays an important role in the function of the central nervous, renal, hormonal and cardiovascular systems. The development of methods for dopamine quantification in blood and biological fluids is the subject of intense current investigation [1–5]. Since dopamine is easily oxidizable, electrochemical methods are an ideal choice for the quantitative determination of dopamine. However, electrochemical oxidation of DA at conventional electrodes is found difficult because

of (a) fouling of the electrode surface due to the adsorption of oxidation products, (b) interference due to the co-existence of ascorbic acid (AA) in the biological fluids, which also undergoes oxidation more or less at the same potential; and (c) also, the concentration of AA is relatively higher than that of DA in these samples ($\sim 10^3$ times higher than DA), which results in poor selectivity and sensitivity for DA detection.

The detection of DA in the presence of excess of AA is a challenging task in electroanalytical research. To develop an ideal sensor system, both sensitivity and selectivity are equally important. Various attempts are reported in the literature to detect DA using electrochemical approaches based on surface coatings [6], carbon paste electrodes [7], self-assembled monolayers

* Corresponding author. Fax: +91 4565 22 7779.

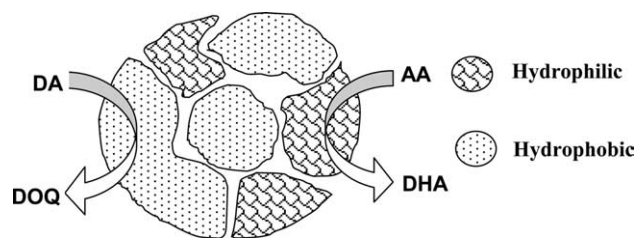
E-mail address: kanalaphani@yahoo.com (K.L.N. Phani).

[8–11], interfaces between two immiscible electrolyte solutions (ITIES) [12], etc. each one associated with its own advantages and limitations.

Deposition of conducting polymers is a simple approach to construct a sensor electrode. The advantages of electropolymerization are that: (a) thin, uniform and adherent polymer films can be obtained; (b) films can be deposited on a small surface area with a high degree of geometrical conformity and controllable thickness using a specific number of growth cycles in potentiodynamic cycling. Among the numerous polymeric materials developed and studied over the past few decades, polyaniline (PANI), polypyrrole (PPy) and poly(3,4-ethylenedioxythiophene) (PEDOT) constitute an important class [13]. PEDOT has received a significant amount of attention as an electrode material for a variety of applications [14,15]. It shows remarkable stability, provides homogeneous films, and can be synthesized electrochemically from both aqueous and non-aqueous media [16–18]. The conductivity of the PEDOT film does not change significantly with the counter ion [19]. Studies on the behaviour of PEDOT in phosphate buffer solutions show a high level of stability when compared to other conducting polymers, suggesting that PEDOT may be a potential candidate for sensor applications and hence it is chosen here for sensing DA.

Simultaneous determination of DA and AA has been reported utilizing electrodes coated with substituted PANIs and PPys, which help separation of the voltammetric signals of DA and AA [20,21]. We found that these approaches lack sensitivity due to the large volumetric capacitance (background) that originates from the polymer film [22], and hence the detectability at submicromolar level becomes difficult. It is natural for one to expect that the sensitivity of the polymer can be increased, by increasing the volume porosity (effective volume) of the film. Nevertheless, there is a *caveat* in this approach in that an increase in film porosity can result in unwanted enhancement in the capacitive currents and render the film mechanically unstable. This higher thickness also limits the mass transport of the analyte molecule (acting as a diffusional barrier). One of the strategies to overcome these limitations is to incorporate an inert high-surface-area material whose content is relatively lower than that of the polymer matrix. An obvious choice is an assembly of gold nanoparticles.

The fabrication of sensors based on nanoparticle incorporated/embedded polymeric matrices are of recent technological interest [23,24]. Arrays of Au nanoparticles have been utilized for electrochemical sensors as they exhibit excellent catalytic activity towards various reactions [25–29]. In these, the Au nanoparticles function efficiently as “electron antennae” [30]. In the present work, we have taken advantage of (a) the hydrophobic/hydrophilic nature of the polymer film; and (b) the signal enhancing character of the embedded



Scheme 1. Depiction of hydrophobic and hydrophilic regions on the conducting polymer film; DOQ = Dopamine-*o*-quinone, DHA = Dehydro ascorbate.

Au nanoparticles. We work with a premise that the polymer film contains a distribution of hydrophobic (reduced) and hydrophilic (oxidized) regions [31] and dopamine prefers to interact with the more hydrophobic regions (Scheme 1).

In the present investigation, we attempt to study the effect of Au nanoparticles in conjunction with PEDOT with the aim of achieving DA determination at nM levels in the presence of mM concentrations of AA.

2. Experimental

2.1. Materials

3,4-ethylenedioxythiophene (EDOT, Baytron M) was a gift sample provided by Bayer AG (Germany). HAuCl_4 (Sigma–Aldrich), dopamine (Acros), ascorbic acid (E-Merck), potassium dihydrogen phosphate (E-Merck), sodium hydroxide (E-Merck) were used as received. The aqueous solutions were prepared using Milli-Q water (18.3Ω) (Millipore).

In the electrochemical experiments, a GC electrode (ϕ 3 mm, BAS, Inc.) and a platinum foil were used as the working and auxiliary electrodes, respectively, in a standard 3-electrode configuration. All the potential values are reported against the standard calomel electrode (SCE) reference unless otherwise mentioned.

2.2. Instrumentation

Electrochemical experiments were carried out using a potentiostat/galvanostat Autolab PGSTAT-30 (Eco-Chemie B.V., The Netherlands) at ambient temperature ($25 \pm 1 \text{ }^\circ\text{C}$). To record the differential pulse voltammograms (DPV), the following input parameters were used: scan rate: 30 mV s^{-1} , sample-width: 17 ms, pulse-amplitude: 50 mV, pulse-width (modulation time): 50 ms, pulse-period (interval): 200 ms and rest-time: 2 s. Peak currents were determined either after subtraction of a manually added baseline or as absolute peak heights above zero.

PEDOT/Au-PEDOT films (coated on ITO glass substrates supplied by Donnelly Corp., USA) were

characterized by atomic force microscopy (Molecular Imaging, USA) using gold coated SiN₃ cantilevers (Force Constant 3 n/W) and a fiber-optic UV–Visible spectrometer (SD 2000, Ocean Optics).

2.3. Methods

2.3.1. Preparation of PEDOT modified GCE

PEDOT was deposited from a solution of 25 mM EDOT + 0.1 M tetrabutylammonium perchlorate in acetonitrile on a glassy carbon electrode by potential scanning between -0.9 and 1.7 V vs. an Ag wire *pseudo*-reference electrode. PEDOT film was allowed to grow on the GCE surface for five successive scans, as seen from the increasing anodic and cathodic peak current densities. The cycling was intentionally limited to five cycles to obtain only thin films.

2.3.2. Preparation of Au-PEDOT ($Au_{\text{nanopedot}}$) composites modified GCE

The biphasic procedure of Brust et al. [32] was followed to prepare the Au particles protected by polymeric/oligomeric species of EDOT ($Au_{\text{nano/edot}}$) using the self-assembling character of thiophenes on gold surfaces [33]. Briefly, an aqueous solution of hydrogen tetrachloroaurate (20 ml, 1 mM) was added to a solution of tetraoctylammonium bromide (TOABr) in toluene (20 ml, 40 mM). The organic layer was separated out after the phase transfer of $AuCl_4^-$. EDOT (25 mM) in toluene was added to this organic phase and the mixture was stirred for 6 h. A freshly prepared aqueous solution of sodium borohydride (20 ml, 10 mM) was added. A wine red colouration of the organic phase was observed indicating the formation of $Au_{\text{nano/edot}}$ MPC. Toluene was evaporated using a rotary evaporator and the resulting residue was washed with acetone three times to remove the stabilizer (TOABr). Then, $Au_{\text{nano/edot}}$ MPC was redissolved in acetonitrile. $Au_{\text{nano/edot}}$ was electrochemically deposited as a continuous film on GCE from a solution of $Au_{\text{nano/edot}}$ MPC in acetonitrile containing tetrabutylammonium perchlorate as supporting electrolyte. The conducting polymer provides a matrix for the nanoparticles.

3. Results and discussion

3.1. Characterization of PEDOT/ $Au_{\text{nanopedot}}$ modified electrodes

Fig. 1 shows the absorption spectra of the PEDOT/ $Au_{\text{nanopedot}}$ film coated on ITO glass substrates. The spectrum obtained for the $Au_{\text{nanopedot}}$ film is very similar to that of the $Au_{\text{nano/edot}}$ MPC though the intensity is relatively small. Both $Au_{\text{nano/edot}}$ MPC and $Au_{\text{nanopedot}}$ give an absorption maximum at ~ 530 and 540 nm that corresponds to a particle size of ~ 20 – 40 nm [25,34].

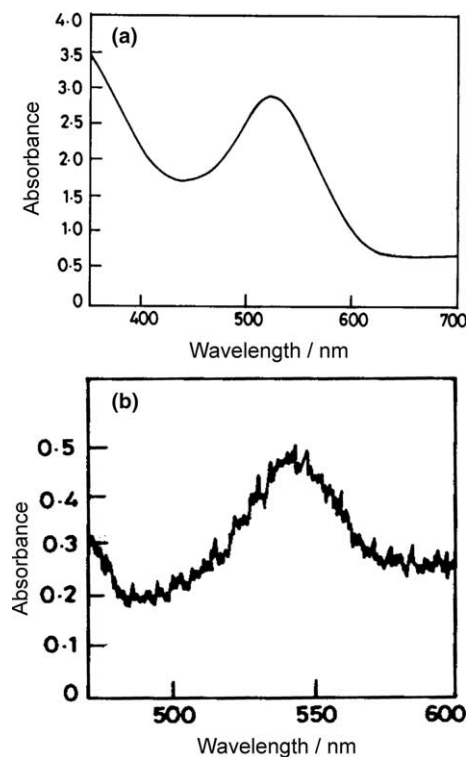


Fig. 1. UV–Vis absorption spectra of: (a) EDOT stabilized Au nanoparticles, (b) Au-nanoparticle incorporated PEDOT film.

The atomic force microscopy (AFM) images (Fig. 2) show the surface morphology and film thickness of the electropolymerised PEDOT film and the $Au_{\text{nano/edot}}$ film coated on ITO glass substrates. The film was obtained by cycling the electrode potential between -0.5 and 1.9 V vs. the Ag wire *pseudo*-reference (five cycles) in the corresponding solution. The topography of PEDOT on the GCE is relatively smooth, with a height variation of ~ 10 nm. The Au clusters are the spherical patches on the PEDOT strands. The image also clearly shows that the Au clusters of 50 – 100 nm sizes are well distributed throughout the polymer matrix. Film thickness measurements, performed with three-dimensional AFM analysis, show a thickness of ~ 100 nm. From the AFM image, the Au-cluster density on the polymer film is found to be ~ 25 per $(1000 \text{ nm} \times 1000 \text{ nm})$.

Fig. 3 shows the cyclic voltammograms of PEDOT and $Au_{\text{nanopedot}}$ coated GCE in 0.5 M sulphuric acid in a potential range of -0.7 to 1.2 V. The CV characteristics of the PEDOT film do not show any characteristic peak within the potential scan range, whereas the Au incorporated polymer film shows the “signature” of the voltammetric behaviour of Au stripping in 0.5 M H_2SO_4 (a weak response at 0.45 V vs. MSE) revealing the presence of Au_{nano} in the film. However, the current response is weak because of masking by the relatively large background current due to the polymer matrix.

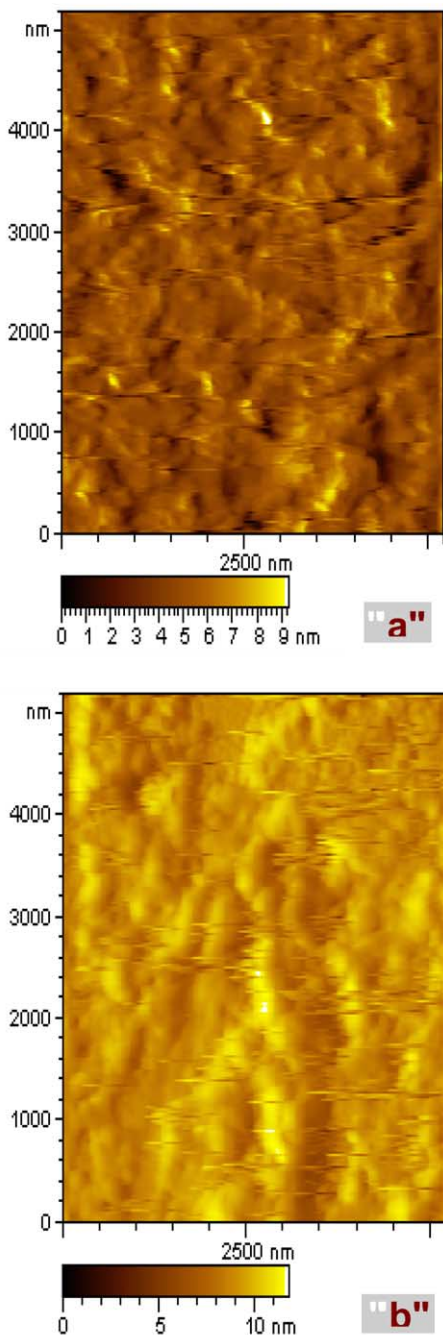


Fig. 2. AFM image of PEDOT and $\text{Au}_{\text{nano/pedot}}$ films coated on a ITO glass.

3.2. Oxidation of DA on PEDOT and $\text{Au}_{\text{nano/pedot}}$ modified electrodes

The oxidation behaviour of dopamine at bare GCE, PEDOT and the $\text{Au}_{\text{nano/pedot}}$ modified GCE is shown in Fig. 4. Oxidation of DA occurs at ~ 0.12 V irrespective of the electrode surface and the modifier. During oxidation, DA undergoes a two-electron oxidation

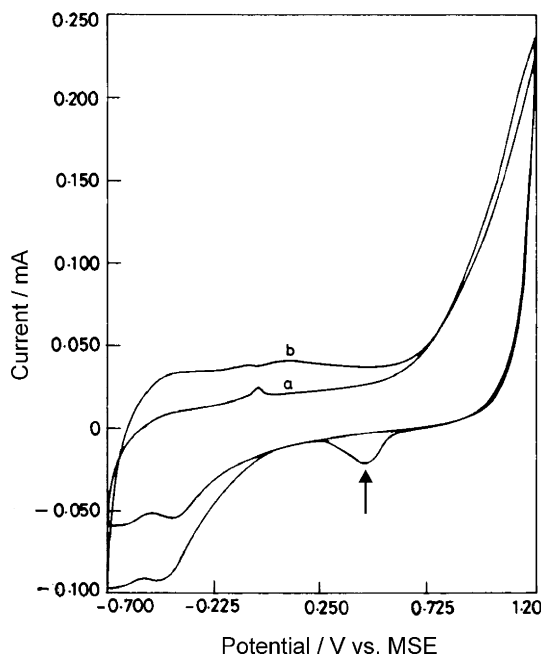


Fig. 3. Redox behaviour of: (a) PEDOT and (b) $\text{Au}_{\text{nano/pedot}}$ coated GCE in 0.5 M sulphuric acid in a potential range of -0.7 to 1.2 V, Scan rate 100 mV s^{-1} (\uparrow mark denotes the reduction of Au).

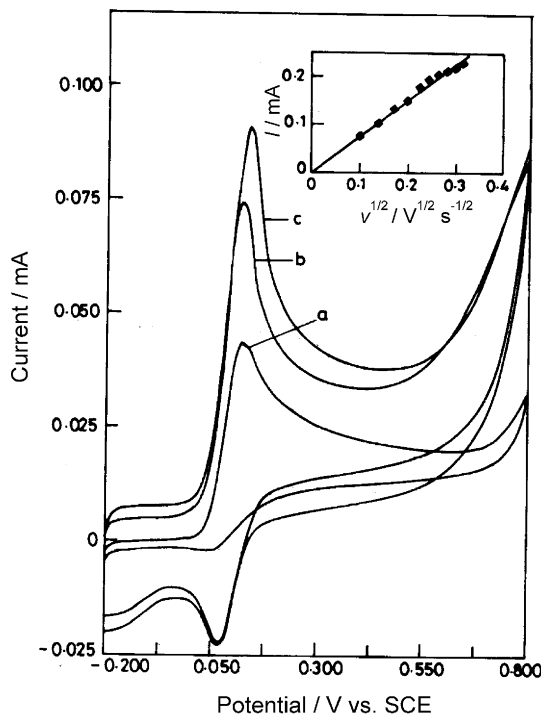


Fig. 4. Cyclic voltammetric behaviour of DA (0.5 mM) at: (a) bare, (b) PEDOT and (c) $\text{Au}_{\text{nano/pedot}}$ coated GC electrodes in PBS of pH 7.4. Scan rate 50 mV s^{-1} . (Inset: relationship between square root of scan rate and peak current.)

where DOQ is the *o*-quinone form of DA. When compared to bare GCE, the oxidation current increases by 33% and 48% on PEDOT and $\text{Au}_{\text{nano/pedot}}$ modified

electrodes, respectively, which clearly indicates catalytic DA oxidation on the modified electrodes. The increase in oxidation current in the presence of Au nanoparticles is attributed to the favourable weak adsorption of DA cations on gold particles [23]. The weak adsorption of DA on the Au surface may be because of the fact that dopamine self-assembles on gold surfaces through the interaction of $-\text{NH}_2$ with Au [35]. Interestingly, the reversibility of DA oxidation is also greatly enhanced on the PEDOT/ $\text{Au}_{\text{nano/pedot}}$ electrode, which may have been favoured by the PEDOT polymer film (since the PEDOT film has a rich electron cloud), that acts as an electron mediator. In addition, a hydrophobic environment appears to favour reversible oxidation of dopamine [36]. The peak separation ($\Delta E_p = |E_{\text{pa}} - E_{\text{pc}}|$) at a scan rate of 0.05 V s^{-1} , is found to be $0.085 \pm 0.002 \text{ V}$ on bare GCE, whereas it is $0.049 \pm 0.002 \text{ V}$ on the PEDOT electrode and $0.060 \pm 0.002 \text{ V}$ on the $\text{Au}_{\text{nano/pedot}}$ electrode, showing faster electron transfer kinetics on PEDOT, as well as on the $\text{Au}_{\text{nano/pedot}}$ film. Further, the linear relationship between the peak current and square root of sweep rate (Fig. 4, inset) in the scan rate range from 0.005 to 0.15 V s^{-1} points to the diffusion-controlled nature of DA oxidation on $\text{Au}_{\text{nano/pedot}}$ films. In addition, the absence of an oxidation current in the cycles subsequent to the first cycles indicates electrode fouling by the oxidation products. Recently, a very high selectivity for DA was reported using exfoliated graphite electrodes [37], and this was attributed to the adsorption of DA. Nevertheless, the I_p vs. $v^{1/2}$ plots showed a non-linear trend and the method appears to be suitable only for adsorptive stripping voltammetry.

3.3. Oxidation of AA on PEDOT/ Au -PEDOT modified electrodes

Fig. 5 shows the oxidation behaviour of AA on bare GC and PEDOT/ $\text{Au}_{\text{nano/pedot}}$ modified GC electrodes. An irreversible oxidation occurs at 0.156 V at bare GCE, whereas it occurs at -0.020 and -0.060 V on PEDOT and $\text{Au}_{\text{nano/pedot}}$ modified electrodes, respectively. An increase of 40% in AA oxidation current is noticed on both PEDOT and $\text{Au}_{\text{nano/pedot}}$ modified electrodes when compared to bare GCE. Thus, both modified electrodes are catalytic towards AA oxidation. The plot of AA oxidation current against square root of scan rate is linear in the range from 0.005 to 0.15 V s^{-1} showing that the AA oxidation process is diffusion-controlled on the $\text{Au}_{\text{nano/pedot}}$ film.

Having examined the individual oxidation behaviour of AA and DA on these three electrodes, details of the interdependence of AA and DA oxidation at the above-modified electrodes are in order. This study is necessitated due to the expected shifts in their peak potential values in each other's presence [3,8,20,38].

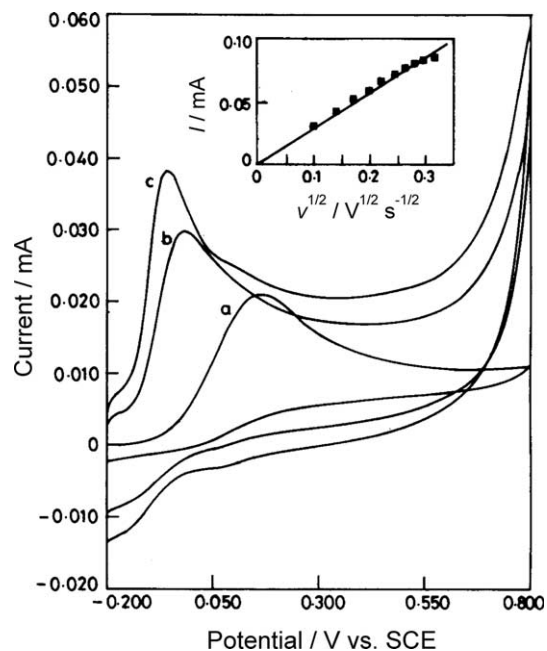


Fig. 5. Cyclic voltammetric behaviour of AA (0.5 mM) at: (a) bare, (b) PEDOT and (c) $\text{Au}_{\text{nano/pedot}}$ coated GC electrodes in phosphate buffer solution (PBS) of pH 7.4. Scan rate 50 mV s^{-1} . (Inset: relationship between square root of scan rate and peak current.)

3.4. Oxidation of DA and AA on PEDOT/ $\text{Au}_{\text{nano/pedot}}$ modified electrodes

Fig. 6 shows the oxidation of co-existing DA and AA on bare GCE, PEDOT, and $\text{Au}_{\text{nano/pedot}}$ modified GC electrodes. It is well known that both DA and AA undergo oxidation at almost the same potential and appear as a single broad peak on a GC electrode [39,40]. However they are clearly separated on a PEDOT-electrode by $\sim 230 \text{ mV}$. On $\text{Au}_{\text{nano/pedot}}$ modified GC electrode also, the same separation of AA and DA oxidation is retained. DA is oxidized at 0.144 (PEDOT)/ 0.127 ($\text{Au}_{\text{nano/pedot}}$) V and AA oxidation occurs at -0.066 (PEDOT)/ -0.060 ($\text{Au}_{\text{nano/pedot}}$) V]. It is interesting to note that the reversibility of DA oxidation is enhanced on both PEDOT- and $\text{Au}_{\text{nano/pedot}}$ modified electrodes, as indicated by the appearance of a peak at 0.073 V in the reverse scan corresponding to the reduction of the oxidized species of DA and a decrease in the ΔE_p values (i.e., 71 and 54 mV , respectively). While Au-incorporation seems to favour reversible oxidation of DA, it also enhances the DA oxidation current magnitudes.

Fig. 7 depicts a histogram presenting a comparison of the behaviour of these electrodes with respect to the oxidation of DA and AA. As can be seen from this figure, the peak current of DA is enhanced in the case of the $\text{Au}_{\text{nano/pedot}}$ electrode compared to that of other electrodes, even in the presence of AA. This clearly shows the synergism between the polymer matrix and the embedded Au nanoparticles.

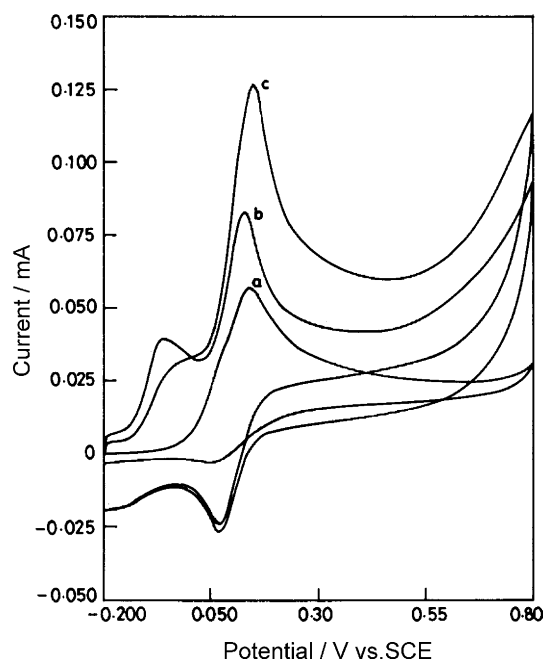


Fig. 6. Cyclic voltammetric behaviour of DA (0.5 mM) + AA (0.5 mM) at: (a) bare, (b) PEDOT and (c) Au_{nano}/pedot coated GC electrodes in PBS of pH 7.4. Scan rate 50 mV s⁻¹.

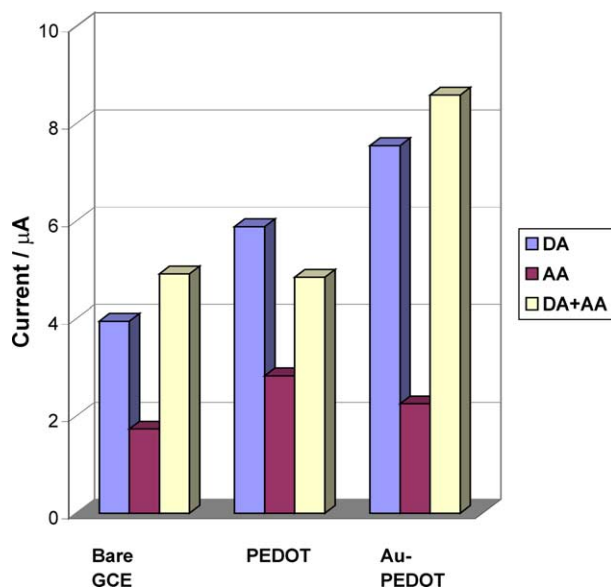


Fig. 7. Histogram comparing the behaviour of bare, PEDOT, Au_{nano}/pedot coated GC electrodes with respect to oxidation of 0.5 mM of DA and AA. (Data taken from CV measurements.)

It is now established through voltammetric studies that the PEDOT polymeric film favours the separation of the voltammetric peaks of DA and AA through hydrophobic/non-specific interactions. It is reasoned that the conducting polymer films (ca. polypyrrole) coated on the electrode surfaces contain a distribution of “reduced” and “oxidized” regions [31,41] and that the reduced regions are more hydrophobic [42] in nat-

ure, and the same is expected in the case of PEDOT. Further, we establish this feature through current sensing atomic force microscopy (CS-AFM) of the PEDOT film that shows clear distinct regions of conducting (oxidized) and non-conducting (reduced) regions (Fig. 8). It may also be stated that DA is more hydrophobic than AA and it is likely that DA interacts with the “reduced” regions of PEDOT through hydrophobic–hydrophobic interactions, whereas AA does not. This is understandable since the “reduced” form of the film acts as a mere redox polymer [21] and can mediate the electron transfer for oxidation of DA. It is also reported that hydrophobicity of the polymer is one of the important factors that is responsible for the selective DA receptor ligand bonding [43]. In the case of AA oxidation, catalytic oxidation is observed as noticed from the shift of potential to less positive values. This may arise because of the electrostatic interactions between the oxidized regions of the film and the anionic AA.

Further, the DA adsorption is favoured by the Au nanoparticles through specific interactions through –NH₂ groups [35]. It is speculated that the Au_{nano} surrounded by a “hydrophobic sheath” tend to reside within these hydrophobic regions of PEDOT and can offer a combined effect of increasing the DA oxidation current.

Thus, in this present study, Au favours the DA adsorption and the use of Au_{nano} results in DA signal enhancement. Yet, the sensitivity of these polymeric modified electrodes towards DA sensing is found to be low due to the presence of a large capacitive current. It is reasonable to expect that increasing the thickness

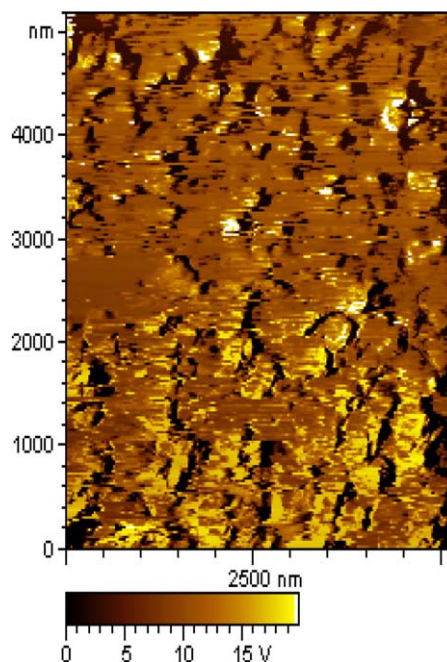


Fig. 8. Current sensing atomic force microscopy (CS-AFM) of PEDOT film.

of the polymer film can enhance the current signal, but thicker films are usually associated with a greater extent of porosity. Increased film thickness also results in unwanted charging current enhancement, thus limiting their detection at submicromolar levels usually with low signal-to-noise ratio (S/N). It is likely that the analyte molecules (DA/AA) can be trapped inside the porous polymeric matrix through specific/non-specific interactions in thicker porous films, limiting the scope of renewal of the surface for repeated analysis (ca. fouling effect). In order to minimize the charging current, the PEDOT film is kept as thin as possible, at the same time ensuring complete coverage of the electrode surface by the PEDOT film. In view of the charging current generated by the polymer film, pulse voltammetric techniques are resorted to in this study to increase the sensitivity [1].

Fig. 9 exhibits the DPVs obtained for varying DA concentrations in the presence of a fixed concentration of AA on PEDOT modified electrodes. The voltammetric peak current of AA oxidation remains unchanged, whereas the oxidation current of DA increases linearly as the bulk concentration of DA is increased. This further confirms that the oxidations of DA and AA at a PEDOT film take place independently. The detection limit of DA in the presence of 1 mM of AA was found to be 2.0 nM. The calibration plot (Fig. 10) for DA is found to be linear with a correlation coefficient (R^2) of 0.97 with a slope value of $0.85 \mu\text{A nM}^{-1}$ for dopamine.

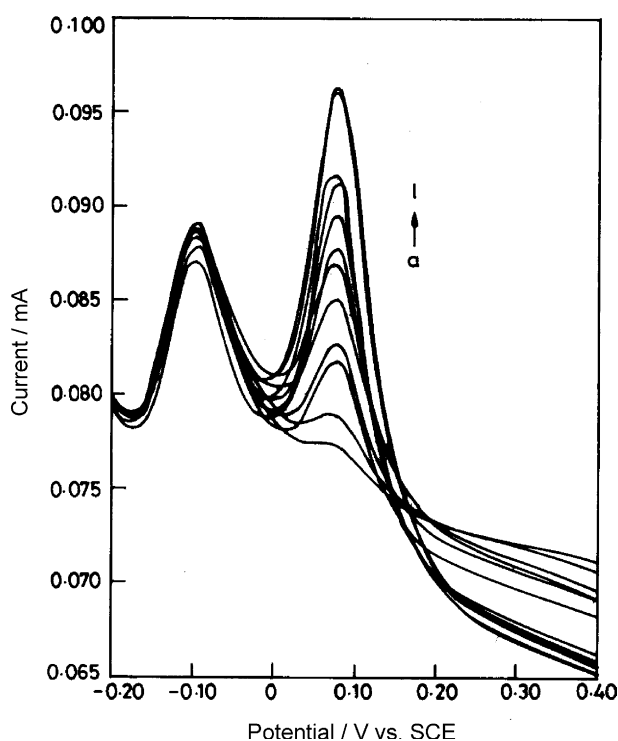


Fig. 9. Differential pulse voltammogram of AA and DA at the $\text{Au}_{\text{nano}}/\text{pedot}$ film coated GC electrode in PBS 7.4 solution. [DA] was changed and [AA] was kept constant (i.e., [AA]: 1 mM; [DA]: (a) 2, (b) 4, (c) 6, (d) 8, (e) 10, (f) 12, (g) 14, (h) 16, (i) 17, (j) 18, (k) 20, (l) 22 nM).

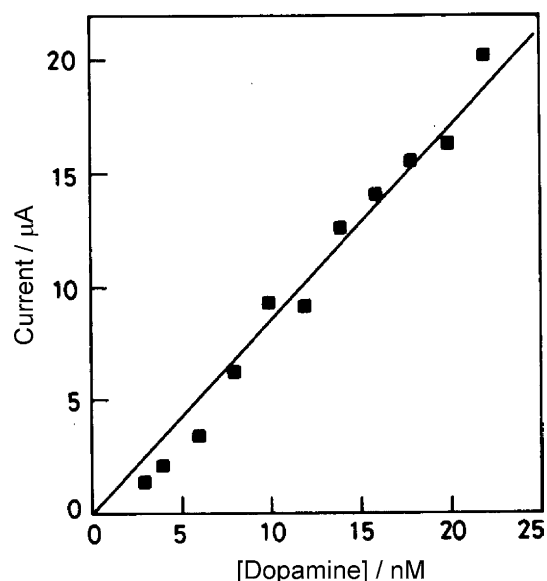


Fig. 10. Relationship between the DA oxidation current and concentration of DA.

Fig. 11 shows the steady state current response obtained for the oxidation of DA at the PEDOT modified electrodes in the presence and absence of 1 mM of AA. The concentration of DA was varied by stepwise addition of $10 \mu\text{l}$ of 10 mM DA into the PBS solution of pH 7.4 and each addition of DA increased the

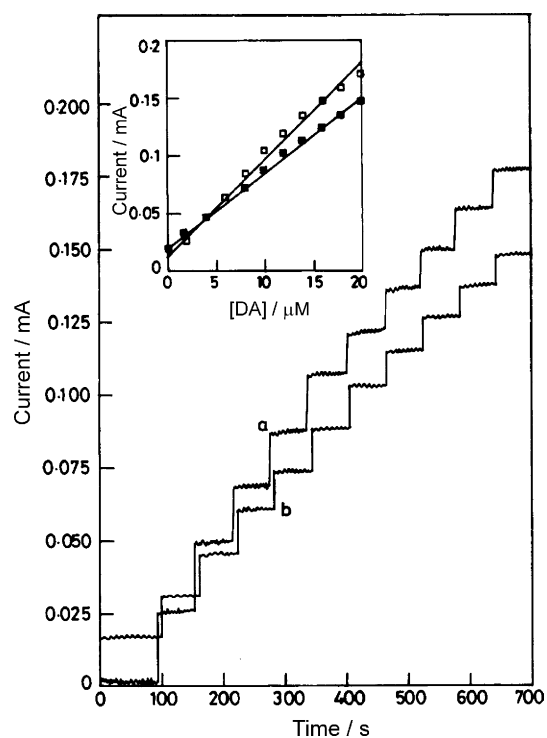


Fig. 11. Steady-state current response for the oxidation of DA at the PEDOT modified electrodes (a) without and (b) with 1 mM of AA. (Inset: relationship between DA concentration and oxidation current.)

concentration of AA by $2\ \mu\text{M}$. The steady-state current for the oxidation of DA in PBS solutions was examined by holding the potential of the electrode at 0.20 V. The current response for the oxidation of DA with and without AA is very similar. Further, a good linear relationship (Fig. 11, inset) between the DA concentration and current magnitude with a correlation coefficient of 0.99 was found for the $\text{Au}_{\text{nano/pedot}}$ electrode. The sensitivity of the $\text{Au}_{\text{nano/pedot}}$ coated electrode towards the DA oxidation was found to be $\sim 6.5\text{--}8.5\ \mu\text{A}\ \mu\text{M}^{-1}$. A stable and rapid current response was obtained within 1–2 s upon repeated addition. This fact confirms the elimination of the oxidation of AA by the modified electrodes and thus the selective determination of DA is possible, irrespective of the presence of AA in large excess. This result is of great significance from the viewpoint of practical applications. Thus, this work demonstrates that both sensitivity and selectivity can be achieved by using composites such as the ones employed here.

The films also appear to be free from fouling by the analytes and/or the oxidized products, as their penetration into the thin film modifier is likely to be minimal (ca. 2%). However, repeated cycling of the electrode in a pH 7.4 buffer is found to remove the incorporated analytes completely, especially DA. The selectivity was found to be consistently reproducible. A series of 20 repetitive voltammetric determinations of sample solutions containing $10\ \mu\text{M}$ of DA and $10\ \mu\text{M}$ of AA was performed to evaluate the stability of the modified electrode over 30 days. The coefficient of variation was found to be $<5\%$, indicating that the modified electrode is not subject to surface fouling by the oxidation product (which was originally known to foul glassy carbon surfaces [44]), whereas a system based polyphenol-modified electrode [45] suffered a loss of up to $\sim 15\%$ in the current output. Unfortunately, very few studies have reported the degree of reproducibility and electrode stability and the information available is at the best very qualitative, thus preventing a systematic quantitative comparison. These advantages accruing from the catalytic function of the film improved the selectivity and sensitivity of the voltammetric determination of DA in the presence of AA.

To ascertain further the reproducibility of the results, three different PEDOT electrodes with and without Au nanoparticles and their responses towards the oxidation of AA and DA were tested. The separation between the voltammetric signals of AA and DA and the sensitivities remained the same at PEDOT electrodes. This confirms the reproducibility of the results. It is pertinent to note that the PEDOT films deposited from aqueous LiClO_4 solutions do not show any selectivity at all between DA and AA, thus indicating that the film morphology apparently plays an important role in the detection of organic molecules [46]. We continue to investigate these systems to elucidate the mechanism of electrooxidation

and the resultant films *vis-à-vis* electrooxidation of organic molecules at these films.

4. Conclusions

In this work, we have demonstrated that the PEDOT polymeric film favours voltammetric peak separation of DA and AA oxidation. Unlike the base electrode, the PEDOT coated GC electrode showed a separation of 230 mV in the oxidation peak potentials of DA and AA present in the same solution. We have also established the possibility of using the Au_{nano} -incorporated PEDOT film modified electrode for improving the sensitivity of DA detection. Incorporation of Au nanoparticles into PEDOT film enhances the DA current signal or in other words, improves the sensitivity. The modified electrodes showed excellent sensitivity, selectivity and anti-fouling properties. Thus, the $\text{Au}_{\text{nano/pedot}}$ incorporated film coated GC electrode could detect DA at 2 nM in the presence of a higher concentration of AA (1 mM), i.e., 1:1000 ratio, which reflects the difference in their concentration under physiological conditions. A good linear relationship between DA concentration and current response was obtained in the concentration range of ca. 0.5 to $2\ \mu\text{M}$. Since PEDOT is proved effective in bringing about a wide separation of the peak potentials of DA and AA, it becomes imperative to study the effect of the dopant anion and density of nanoparticle incorporation on both sensitivity and selectivity in their determination and work is in progress to elucidate these aspects.

Acknowledgements

The authors thank the Department of Science & Technology, New Delhi for a research grant (Interfacial Charge Transfer and Electrocatalytic Characteristics of Metal-filled Matrices, SP/S1/H-20/99).

References

- [1] B.G. Venton, R.M. Wightman, *Anal. Chem.* 75 (2003) 414A.
- [2] L. Zhang, Y.-G. Sun, *Anal. Sci.* 17 (2001) 939.
- [3] X.-L. Wen, Y.-H. Jia, Z.-Li. Liu, *Talanta* 50 (1999) 1027.
- [4] J. Wang, A. Walcarius, *J. Electroanal. Chem.* 407 (1996) 183.
- [5] M. Ferreira, L.R. Dinelli, K. Wohnrath, A.A. Batista, O.N. Oliveira Jr., *Thin Film Solids* 446 (2004) 301.
- [6] J. Wang, P. Tuzhi, *Anal. Chem.* 58 (1986) 3257.
- [7] J. Oni, T. Nyokong, *Anal. Chim. Acta* 434 (2001) 9.
- [8] A. Dalmia, C.C. Liu, R.F. Savinell, *J. Electroanal. Chem.* 430 (1997) 205.
- [9] M.A. Chen, H.L. Li, *Electroanalysis* 10 (1998) 477.
- [10] F. Malem, D. Mandler, *Anal. Chem.* 65 (1993) 37.
- [11] C.R. Raj, K. Tokuda, T. Ohsaka, *Bioelectrochemistry* 53 (2001) 183.

- [12] D.W.A. Arrigan, M. Ghita, V. Beni, *Chem. Commun.* (2004) 732.
- [13] H.B. Mark, N. Atta, K.L. Petticrew, H. Zimmer, Y. Shi, S.K. Lunsford, J.F. Rubinson, A. Galal, *Bioelectrochem. Bioenerg.* 38 (1995) 229.
- [14] K. Krishnamoorthy, R.S. Gokhale, A.Q. Contractor, A. Kumar, *Chem. Commun.* (2004) 820.
- [15] H. Yamato, M. Ohwa, W. Wernet, *J. Electroanal. Chem.* 397 (1995) 163.
- [16] A. Sakmeche, J.J. Aaron, M. Fall, A. Aeiyaich, M. Jouini, J.C. Lacroix, P.C. Lacaze, *Chem. Commun.* (1996) 2723.
- [17] V.S. Vasantha, K.L.N. Phani, *J. Electroanal. Chem.* 520 (2002) 79.
- [18] M. Dietrich, J. Heinze, G. Heywang, F. Jonas, *J. Electroanal. Chem.* 369 (1994) 87.
- [19] L.B. Groenendaal, G. Zotti, P.-H. Aubert, S.M. Waybright, J.R. Reynolds, *Adv. Mater.* 15 (2003) 855.
- [20] P.R. Roy, T. Okajima, T. Ohsaka, *J. Electroanal. Chem.* 561 (2004) 75.
- [21] Z. Gao, H. Huang, *Chem. Commun.* (1998) 2107.
- [22] Z. Cai, C.R. Martin, *J. Electroanal. Chem.* 300 (1991) 35.
- [23] C.R. Raj, T. Okajima, T. Ohsaka, *J. Electroanal. Chem.* 543 (2003) 127.
- [24] R. Gangopadhyay, A. De, *Chem. Mater.* 12 (2000) 608.
- [25] M. Haruta, M. Date, *Appl. Catal. A* 222 (2001) 42.
- [26] A. Doron, E. Katz, I. Willner, *Langmuir* 11 (1995) 1313.
- [27] S.G. Penn, L. Hey, M.J. Natan, *Curr. Opin. Chem. Biol.* 7 (2003) 609.
- [28] P. Alivisatos, *Nat. Biotechnol.* 22 (2004) 47.
- [29] A.N. Shipway, E. Katz, I. Willner, *Chem. Phys. Chem.* 1 (2000) 18.
- [30] K.R. Brown, A.P. Fox, M.J. Natan, *J. Am. Chem. Soc.* 118 (1996) 1154.
- [31] C.R. Martin, L.S. Van Dyke, in: R.W. Murray (Ed.), *Molecular Design of Electrode Surfaces*, Wiley, New York, 1992, pp. 403–424.
- [32] M. Brust, M. Walkes, D. Bethell, D.J. Schiffrin, R. Whyman, *J. Chem. Soc., Chem. Commun.* (1994) 801.
- [33] J. Noh, E. Ito, K. Nakajima, J. Kim, H. Lee, M. Hara, *J. Phys. Chem. B* 106 (2002) 7139.
- [34] K.R. Brown, D.G. Walter, M. Natan, *J. Chem. Mater.* 12 (2000) 306.
- [35] Highlights from recent literature, *Gold Bulletin*, 36 (2003) 65.
- [36] X.-L. Wen, Y.-H. Jia, Z.-L. Liu, *Talanta* 50 (1999) 1027.
- [37] P. Ramesh, G.S. Suresh, S. Sampath, *J. Electroanal. Chem.* 561 (2004) 173.
- [38] T. Selvaraju, R. Ramaraj, *J. Appl. Electrochem.* 33 (2003) 759.
- [39] J. Mathiyarasu, S. Senthil Kumar, K.L.N. Phani, V. Yegnaraman, *J. Appl. Electrochem.* (2005) in press.
- [40] P.R. Roy, T. Okajima, T. Ohsaka, *Bioelectrochemistry* 59 (2003) 11.
- [41] M.E.G. Lyons, in: M.E.G. Lyons (Ed.), *Electroactive Polymer Electrochemistry, Part I*, Plenum Press, New York, 1994, pp. 65–116.
- [42] G. Schopf, G. Koßmehl, *Polythiophenes – Electrically Conductive Polymers*, Springer, Germany, 1997, p. 80.
- [43] R.G.A. Bone, H.O. Villar, *J. Mol. Graph.* 13 (1995) 201.
- [44] R.F. Lane, A.T. Hubbard, *Anal. Chem.* 48 (1976) 1287.
- [45] A. Ciszewski, G. Milczarek, *Anal. Chem.* 71 (1999) 1055.
- [46] S. Senthil Kumar, Unpublished results.